New Materials, Compounds and Applications
Vol.9, No.2, 2025, pp.254-270
https://doi.org/10.62476/nmca.92254

INVESTIGATION ON THE INFLUENCE OF PROCESS PARAMETERS ON THE MECHANICAL PERFORMANCE OF 3D PRINTED SPECIMENS

Ganesh Radhakrishnan[1*], Teodora Odett Breaz[2], Sulaiman Khamis Sulaiman Al Gharibi[1], Salim Said Mohammed Al Abri[1], Majid Saleh Sulaiman Al Abri[1], Ahmed Mohammed Said Al Shaqsi[1], Al Muataman Ali Saleh Al Abri[1], Bashar Nasrullah Salim Al Abri[1], Ibrahim Abdallah Harib Al Awimari[1], Kadhavoor R. Karthikeyan[3]

[1]Mechanical Engineering, College of Engineering & Technology, University of Technology and Applied Sciences, Nizwa, Oman
[2]Department of Business Administration and Marketing, "1 Decembrie 1918" University of Alba Iulia, Alba Iulia, Romania
[3]Department of Applied Mathematics and Science, National University of Science and Technology, Muscat, Oman

Abstract. 3D printing using Fused Deposition Modeling (FDM) is a familiar technique in additive manufacturing employed in this work to fabricate specimens made of Polylactic Acid (PLA). The objective of the present study is to investigate the mechanical behavior of 3D printed PLA specimens for various testing parameters combination. The process parameters selected for investigation in this study were the infill pattern, filling speed and layer thickness, whereas parameters such as the infill density, raster angle, build orientation and nozzle temperature were maintained at a fixed value during fabrication. Analyzing the 3D printed specimens, higher order porosity was observed at layer thickness 0.28 mm and filling speed 50 mm/s. The tensile strength increased with increasing filling speed and decreasing filling layer thickness. A maximum tensile strength of approximately 15 MPa was observed for a filling speed of 50 mm/s and layer thickness 0.16 mm. The tensile performance of the specimens with gyroid filling patterns was inferior to that of the specimens with line and triangular filling patterns. Specimens fabricated with filling speed of 30 mm/s and filling layer thickness of 0.16 mm resulted in better compressive strength. The flexural performance of 3D printed specimens was better at higher filling speeds, which contradicted the tensile and compression performances. Overall, specimens printed under lesser filling speed of 30 mm/s and lesser layer thickness of 0.16 mm resulted in better mechanical performance due to enhanced bonding strength with higher degree of adhesion between the layers.

Keywords: *3D printing, Polylactic acid, infill pattern, filling speed, layer thickness, tensile strength.*

Corresponding Author: *Ganesh Radhakrishnan, Mechanical Engineering, College of Engineering & Technology, University of Technology and Applied Sciences, Nizwa, Oman,*
e-mail: ganesh.radhakrishnan@utas.edu.om

Received: *8 April 2025;* ***Accepted:*** *20 June 2025;* ***Published:*** *5 August 2025.*

1. Introduction

Additive manufacturing, also known as 3D printing, is the process of creating three-dimensional objects by adding materials layer by layer. It is a revolutionary manufacturing technique that enables the creation of complex geometries and intricate designs that are difficult or impossible to produce using traditional manufacturing methods. Various additive manufacturing technologies exist, but they all share the basic principle of adding materials layer by layer to build up the final object. The most common approach involves melting or softening a material, such as plastic or metal and depositing it in thin layers, which solidify to form a desired shape. This can be achieved using techniques such as fused deposition modeling (FDM) for plastics or selective laser melting (SLM) for metals. Traditional manufacturing methods often involve subtractive processes, in which the material is removed from a solid block to achieve the desired shape. In contrast, additive manufacturing allows for the direct creation of the final object, reducing waste and enabling more design freedom (Kun, 2016). One of the most often used materials in 3D printing is PLA (Poly Lactic Acid). It is well-liked by professionals, academics and amateurs because of its simplicity, accessibility and eco-friendliness. Compared to other 3D printing materials, PLA is biodegradable and more ecologically friendly because it is made from renewable resources such as cornstarch or sugarcane. PLA is well known for its simplicity to print. This makes printing easier because a heated print bed is unnecessary. Painter tape and print beds coated with glue or adhesives are two more surfaces to which PLA sticks well. Liu et al. (2023) recommended a 41% triangular fill for the supporting part and they verified its suitability under a compressiveload of 1225 N. Further, they provided insights for other applications requiring compressive strength in 3D printing. The mechanical properties based on the impact of the infill density on 3D-printed part was well-documented. It generally well known that higherinfill densities enhance strength when other parameters are treated as constant. This study examined the impact of infill parameters on the compressive strength of 3D-printed carbon fiber-reinforced nylon. In addition, we evaluated the infill pattern (triangular, rectangular and gyroid) and infill density's influence on mass. Triangular infill outperformed the other infill patterns, with higher mass yielding greater strength. The influence of thickness on the mechanical behavior of components produced through fused deposition modeling technology using Polylactic Acid (PLA) was studied by Xu et al. (2021). The team used 2D digital image correlation (DIC) to evaluate the displacement and strain on the specimen surfaces and examined the fractographs using optical microscopy to understand the failure mechanisms. The findings indicated that thicker specimens exhibited higher ultimate tensile strength and elongation at failure and thicker specimens also showed less variation in elongation at failure owing to reduced temperature distribution effects on the building plate. The interlayer bonding strength of 3D Printed PEEK Specimens was studied by Liaw et al. (2021). Their study explored how printing parameters such as nozzle temperature influences the bonding strength. The nozzle temperature significantly enhanced the bonding strength whereas thermal annealing had a minimal effect. A three-point flexural test was utilized and the study also assessed the interlayer bonding strength in 3D printed PEEK, where force was applied along the layer interface. This approach eliminates the need for post- processing and ensures interlayer fracture. They found that layer height was the sole significant factor that concerns the flexural modulus. Note that modulus decreases as layer height increases. The decrease in flexural modulus is mainly attributed to the formation of voids in thickerlayers. The inverse relationship between the layer thickness and number of printed layers also plays a role. Interestingly, the layer height was the only factor influencing the modulus, with temperature-related parameters such as nozzle temperature and wait time having no significant impact. Mirkhalaf and Fagerstrom (2021) investigated the mechanical behavior of Polylactic acid (PLA) films. Thin PLA films were created by hot pressing and tensile tests were conducted at different strain rates. An elasto-viscoplastic constitutive model was adopted and calibrated to accurately model the mechanical behavior of PLA's, including post-yield softening, under uniaxial stress conditions. Experiments were conducted on the PLA films, revealing their rate-dependent behavior. A viscoelastic model was adopted to predict the mechanical behavior of PLA's and the material properties were quantified. The model successfully captured all deformation regimes, including post-yield softening, under uniaxial tension and the strain-rate dependency of PLA was accurately represented. Numerical and experimental analysis were performed by Nagaraju et al. (2023) on 3D printed specimens for building components obtained through fused deposition modeling (FDM) and stereolithography (SLA) processes. They emphasized various limitations of FDM process such as delamination, wrapping and cracking defects. The mechanical performance of the 3D printed specimens was better in the case of stereolithography than that of fused deposition modeling. Faidallah et al. (2025) analyzed the tensile and compressive behavior of 3D printed carbon fiber reinforced polymer composites. The specimens were fabricated in flat and on-edge orientations. The findings revealed that the addition of carbon fibers significantly reduced the tensile and compressive strength. Fused deposition modeling is viewed as a sustainable advancement in the field of additive manufacturing in terms of economic and material usage.

From the detailed literature review on the 3D printing of PLA specimens through FDM and other techniques, some important findings were drawn and listed as follows. The triangular infill pattern exhibited a superior performance in-terms of mass-related strength. A greater thickness led to a higher tensile strength and elongation at failure, with improved bonding between layers and reduced standard deviation in mechanical properties. From the three infill patterns (triangular, rectangular and gyroid), the triangular infill outperforms the other infill patterns yielding higher mass and greater strength. The thickness can influence the properties of the specimens, with thicker specimens exhibiting a higher ultimate tensile strength and elongation at failure. The Young's modulus decreased slightly when thickness was increased, indicating a reduced stiffness. The printing speed significantly affected the quality of the FDM 3D-printed PLA samples. The influence of various degradation factors on the mechanical behavior of 3D printed specimens prepared by Fused Filament Fabrication (FFF) technology was studied by Sedlak et al. (2023). The mechanical characterization was carried out before and after the degradation. Light, temperature, oxygen and water were considered as degradation factors in the study. Comparing the degradation effect on the mechanical behavior, Acrylonitrile Styrene Acrylate (ASA) proved to be better than Polyethylene Terephthalate Glycol (PETG) and Polylactic acid (PLA). Lanzotti et al. (2015) investigated the influence of process parameters such as layer thickness, infill orientation and number of shell perimeters on the mechanical performance of PLA specimens printed by Fused Deposition Modeling (FDM) technique. Response Surface Methodology (RSM) was used by the team to develop an empirical model with the influential factors as variables for each performance measure in the mechanical characterization. They concluded finally that the process parameter, layer thickness was most influential factor among all other factors considered in the investigation.

Inspite of significant contribution by various researchers worldwide in 3D printing, an ample opportunity exists to explore several research outcomes in terms of challenges and applications of 3D printed products. In most of the research works done so far, the important parameters chosen for investigation are infill density, infill pattern, orientation etc. In view of this, this work was designed with a combination of parameters such as filling speed, infill pattern and layer thickness, while the bed and nozzle temperature were maintained constant during the experimentation. The highlight of this study is that the unique selection of process parameters and in particular the infill patterns chosen for the printing such as line, triangle and gyroid, targeting for a comprehensive analysis and in turn useful scientific outcomes from the study. This parameters combination not only result in fruitful outcomes but also results in certain advances in knowledge enrichment for producing versatile 3D printed products for real time applications. Also, in most of the research work discussed in the literature, mechanical characterization was limited to tensile behavior of the 3D printed specimens, whereas in the present investigation, the 3D printed specimens are subjected to compression and flexural analysis in order to support for the applications targeting for these kind of loads. Hence, an attempt was made to study the influence of certain important process parameters on the mechanical performance of PLA specimens fabricated through the FDM technique in order to further explore the challenges and results with a different combination of process parameters and levels. The details of the experiment and results obtained will be discussed in the following sections.

2. Experimentation

The material selected for 3D printing was Polylactic acid (PLA), brand - iSANMATE, colour - green & Ø 1.75 mm. The properties of PLA were listed in Table 1. Polylactic acid was a thermoplastic monomer derived from renewable organic sources, such as corn starch or sugar cane. The specimens were fabricated using a 3D printer (Ender 3 v2), employing the fusion deposition modeling technique, as shown in Figure 1. The various parameters considered and their levels during the 3D printing are listed in Table 2. The parameters were chosen based on their influence on the mechanical performance of 3D printed specimens. Many researchers and academicians working in the field of additive manufacturing have reported that although there are numerous parameters that affect the quality and performance of 3D printed specimens irrespective of the materials used for printing, the parameters considered in this study were highly significant not only in the quality of printing but also in the strength of the printed specimens. The levels were chosen based on the degree of influence on the mechanical performance as explored through the literature review and specifications of the 3D printer used in the study. The parameters that were treated as constant during fabrication are as follows:

- Infill density: 50 %;
- Room temperature:~25°C (Controlled in a closed environment with less than 10% humidity);
- Nozzle temperature: 210°C;
- Degree of print: 90° (along z axis).

Table 1. Properties of PLA

S.No.	Property	Value
1	Density	1.24 g/cm^3
2	Tensile strength	50 MPa
3	Flexural strength	80 MPa
4	Izod impact strength (unnotched)	96 J/m
5	Shrink rate	0.37-0.4 %

The step-by-step procedure for the fabrication of 3D printed specimens is stated below.

1. Select prepare.
2. Choose autosome option, to balance the bed of 3D printer.
3. Wait until reach at zero level (home position).
4. Balance the bed, make sure the gap between the nozzle and bed was ~0.02 mm.
5. Select disable stepper, to balance all four corners and center of bed.
6. After balance, select preheat PLA.
7. Apply some glue (Elmer's disappearing) in bed, to stick the first layer properly while printing.
8. Wait to reach the temperature of 200°C, at nozzle and 60°C, at bed.
9. After reaching the ambient temperature select print command.
10. See the first layer if it is stuck in bed. If it is not struck in bed repeat the balance again.

Table 2. Process parameters and their levels

PARAMETERS	LEVEL		
	1	2	3
Filling Speed (mm/s)	30	40	50
Infill Pattern	line	triangle	gyroid
Layer thickness (mm)	0.16	0.2	0.28

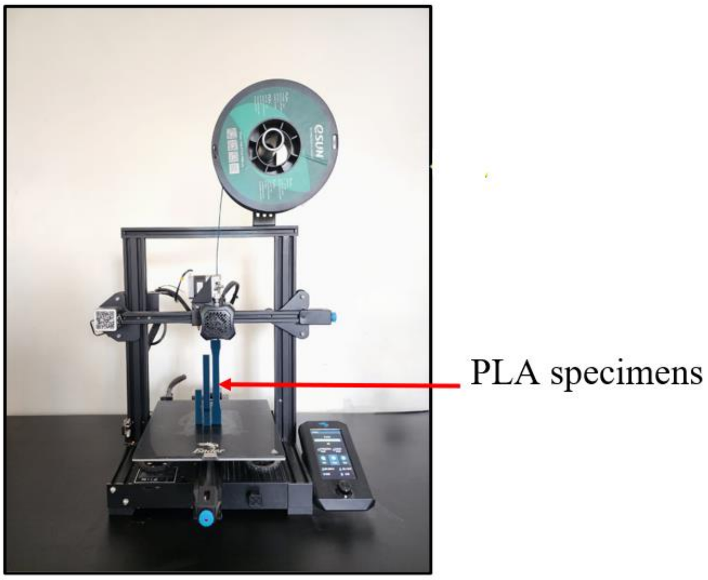

Figure 1. 3D printer machine set-up

The fabricated PLA 3D printed specimens were subjected to physical and mechanical characterization, which included the measurement of properties such as porosity, tensile strength, compressive strength and flexural strength. The influences of the process parameters, filling speed, infill pattern and filling layer thickness considered during printing on the physical and mechanical behavior were analyzed in detail. The porosity of the 3D printed specimens were calculated using Equation 1.

$$\text{Porosity} = \frac{V_T - V_P}{V_T} \times 100\%, \quad (1)$$

where V_T = Theoretical volume of the specimen in m^3 and V_P = Printed volume of the specimen in m^3.

The tensile, compression and flexural tests of the 3D printed specimens were carried out in a Universal Testing Machine (UTM) according to ASTM standards ASTM D638, ASTM D695 and ASTM D790 respectively. Each test was repeated thrice and the average value was taken to ensure the accuracy and consistency of the results. The stress and strain values during tensile and compression tests and the load and deflection during the flexural test were recorded using Data Acquisition (DAQ) system. The ultimate tensile strength, modulus of elasticity, compressive strength and critical flexural loading capacity were computed from the stress-strain diagram obtained from each test. The experimental set-ups for tensile, compression and flexural test are shown in Figure 2 a-c. A strain rate of 0.02 s^{-1} was maintained during the tensile test.

Figure 2. Experimental set ups of (a) tension test (b) compression test and (c) flexural test

The length of the tensile test specimen was 165 mm, with gauge length and gripping lengths of 72 mm and 115 mm respectively. The compression test has a square cross section of side 12.7 mm with a lateral-to-longitudinal dimension ratio of 1:2. The flexural test specimen measured 125 mm in length with a support span of 100 mm and three-point bending with a concentrated load was applied to the specimen at the mid-span. The salient results of the mechanical and physical behavior of 3D printed specimens are detailed in the next section.

3. Results and Discussions

The 3D printed specimens were successfully fabricated with a combination of process parameters at different levels. The cross section of the fabricated specimens is shown in Figure 3 illustrates the infill pattern from a better perspective.

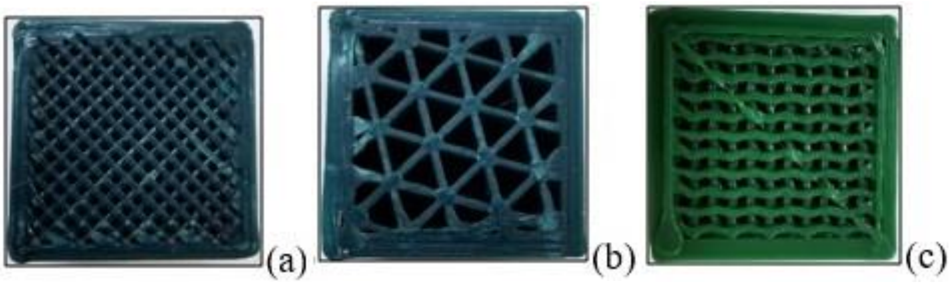

Figure 3. Cross section of fabricated 3D printed specimens (a) line (b) triangle and (c) gyroid

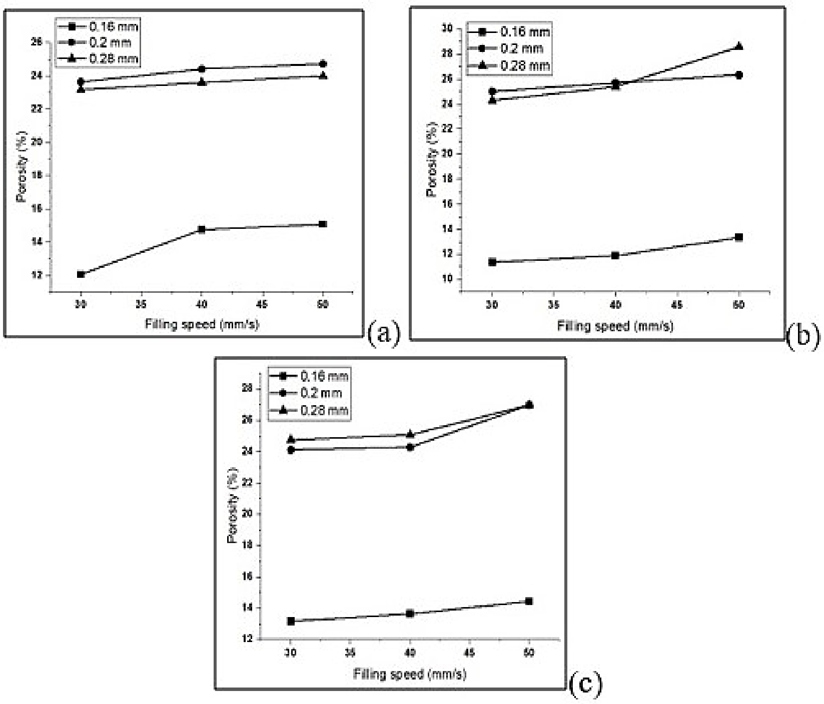

Figure 4. Porosity of 3D printed specimens (a) line (b) triangle and (c) gyroid

The influence of filling speed and layer thickness on the porosity of fabricated specimens for various infill patterns was shown in Figure 4. A significant increase in porosity was observed for the filling speed increasing from 30 to 40 mm/s, whereas for the increase in velocity from 40 to 50 mms, there was only a marginal rise in porosity. Influence of layer thickness on the porosity complemented the impact of filling speed for all the infill patterns (Letcher & Waytashek, 2014; Misran *et al*., 2019). Higher order porosity was observed at layer thickness 0.28 mm and filling speed 50 mm/s.

The observations obtained during the tensile test of 3D printed specimens are shown in Figure 5 a-c for the line, triangle and gyroid filling patterns respectively. In the case of 3D printed specimens with a line pattern, an appreciable transition from ductile to brittle characteristics was observed. With an increase in the filling speed from 30 mm/s to 50 mm/s, the transition of ductile to brittle is considered significant (Hodžić *et al*., 2020; Liu *et al*., 2017; Farbman & McCoy, 2016). The tensile strength increased with an increase in filling speed and decrease in filling layer thickness. The least tensile strength of around 7 MPa was observed for the specimen fabricated with lowest filling speed of 30 mm/s and the least filling layer thickness of 0.16 mm. On the other hand, a maximum tensile strength of 15 MPa was observed for filling speed of 50 mm/s and a layer thickness 0.16 mm. An increase in the filling speed during printing reduced the adhesion between the layers and in turn changes the behavior of the specimen from plastic to elastic. A higher layer thickness and lower filling speed resulted in good adhesion between the layers and increased the plasticity of the printed specimen (Hanon *et al*., 2021). The failure strain was significantly reduced from 0.016 to 0.006 with an increase in the filling speed from 30 mm/s to 50 mm/s and a decrease in the layer thickness from 0.278 to 0.16 mm respectively. Compared with that of the line pattern, the tensile performance of 3D printed specimens with a triangular pattern was appreciably higher. The ultimate tensile strength ranged between 6 to 14 MPa for the line pattern, whereas in case of triangular pattern, it ranged somewhere between 8 to 16 MPa. This was mainly due to the increased adhesion in triangular pattern when compared with that of line pattern, reported by other researchers too in their work (Naik & Thakur, 2021). It was observed that, the time for printing specimens with the line infill pattern was lower than that was required for triangular infill pattern. Faster printing results in weaker part owing to its inferior infill density. This, in turn, resulted in a poor resistance against the tensile loading of the 3D printed specimens.

The trend of the stress-strain relationship was similar for both the filling patterns – line and triangle, but a significant improvement in tensile strength was observed for triangular infill pattern. The specimen with a filling speed 50 mm/s and a layer thickness 0.16 mm resulted in a failure strength of 18 MPa, which was about 20% higher than that of a similar specimen with line filling pattern. From the results of tensile performance of 3D printed specimens with the gyroid filling pattern, it was clear that the tensile performance was lower than that of the line and triangular filling patterns. Many specimens with gyroid patterns exhibited very poor tensile strength of around 5 to 8 MPa. A specific observation in gyroid pattern is that influence of layer thickness on tensile performance was slightly higher than that of filling speed. In gyroid pattern 3D printed specimens, least layer thickness 0.16 mm resulted in better adhesion between the layers which is attributed to the pattern geometry, which was similar to that of results reported by other researchers but they have not considered the gyroid pattern (Kamer *et al*., 2022; Oksiuta *et al*., 2020). The ultimate tensile strength, shown in Figure 6 a-c for all the infill patterns steadily increases with filling speed from 30 mm/s to 50 mm/s for the layer thickness 0.16 mm, whereas for the other layer thicknesses, a marginal drop was observed on the tensile strength for the increase in speed from 40 mm/s to 50 mm/s. Higher layer thickness loses its adhesion behavior at higher filling speeds due to longer wait time, which substantially reduces the temperature and thereby adhesion between the layers. A higher order tensile strength was obtained with triangular filling pattern compared to that of other filling patterns considered in the study. The failure mode in all the tensile specimens is brittle fracture, which was clearly evident from the stress-strain graphs. For example, a tensile specimen, fabricated with triangular infill pattern, 0.16 mm layer thickness and 50 mm/s filling speed with brittle fracture was shown in Figure 7. PLA has very low crystallinity as well as low glass transition temperature and no abnormalities observed during the test. The visco-elastic behavior of the 3D printed specimens revealed a fact that the behavioral change from plastic to elastic was more for line and triangular patterns compared to that of gyroid pattern. At lower infill thickness and at higher infill speed, it was observed a very lower order strain due to lower rate of diffusion. On the other side, at higher infill thickness and lower infill speed, there was substantial route and time for diffusion resulted in higher order strain with more plasticity.

The modulus of elasticity obtained for the specimens was shown in Figure 8 a-c corresponding to line, triangular and gyroid filling pattern respectively. Specimens fabricated with layer thickness 0.16 mm resulted in higher modulus of elasticity than that of other thickness irrespective of the filling pattern. Layer thickness has a negative effect on the modulus of elasticity for all filling speeds. The range of elastic modulus at all filling speeds and layer thickness seems to be in higher order for triangular pattern than that of other patterns. This observation of elastic modulus complemented the results of tensile strength. The stress-strain behavior of 3D printed specimens under compression for various filling speeds, filling layer thickness and infill patterns was shown in Figure 9 a-c. It was observed from the stress-strain behavior that the ultimate compressive strength ranges between 40 to 50 MPa for specimens with triangular infill pattern, whereas for the other infill patterns such as line and gyroid, the compressive strength ranges between 30 to 40 MPa.

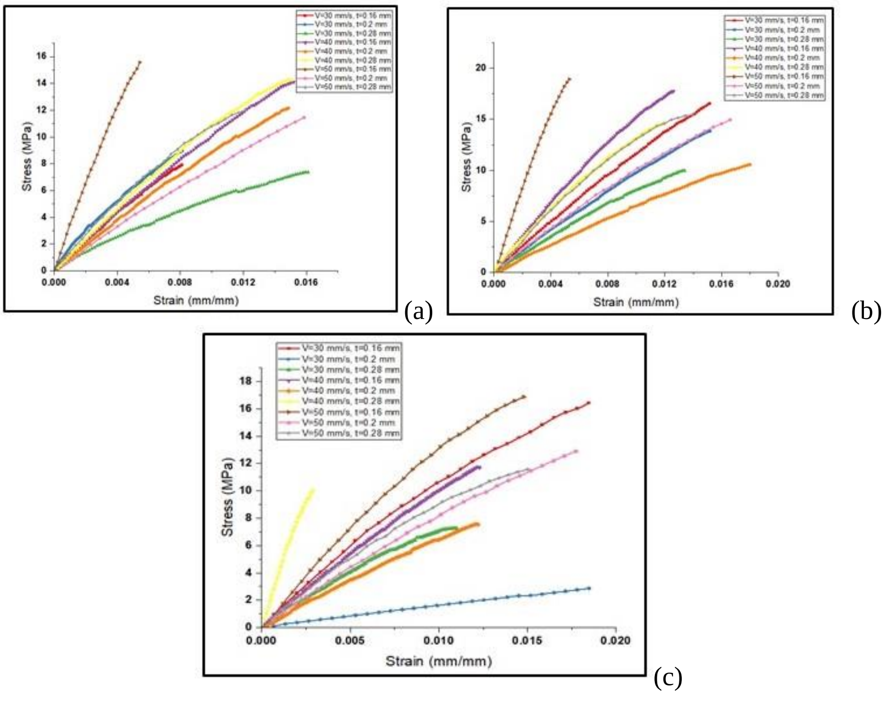

Figure 5. Stress-strain behavior of 3D printed specimens (a) line (b) triangle and (c) gyroid

Appreciable higher order plasticity was obtained for line and gyroid infill patterns and it was significantly reduced in case of triangular pattern. This may be attributed to the fact that the interlocking capacity and denser structure was significantly higher in triangular patterns compared to that of other infill patterns (Geng *et al*., 2019). Increase in filling speed and filling layer thickness drastically reduced the compressive strength, of the specimens, shown in Figure 10. Specimens fabricated with filling speed of 30 mm/s and filling layer thickness of 0.16 mm resulted in better compressive strength that that of higher values of filling speed and filling layer thickness for all infill patterns (Khan *et al*., 2018; Al Khawaja *et al*., 2020).

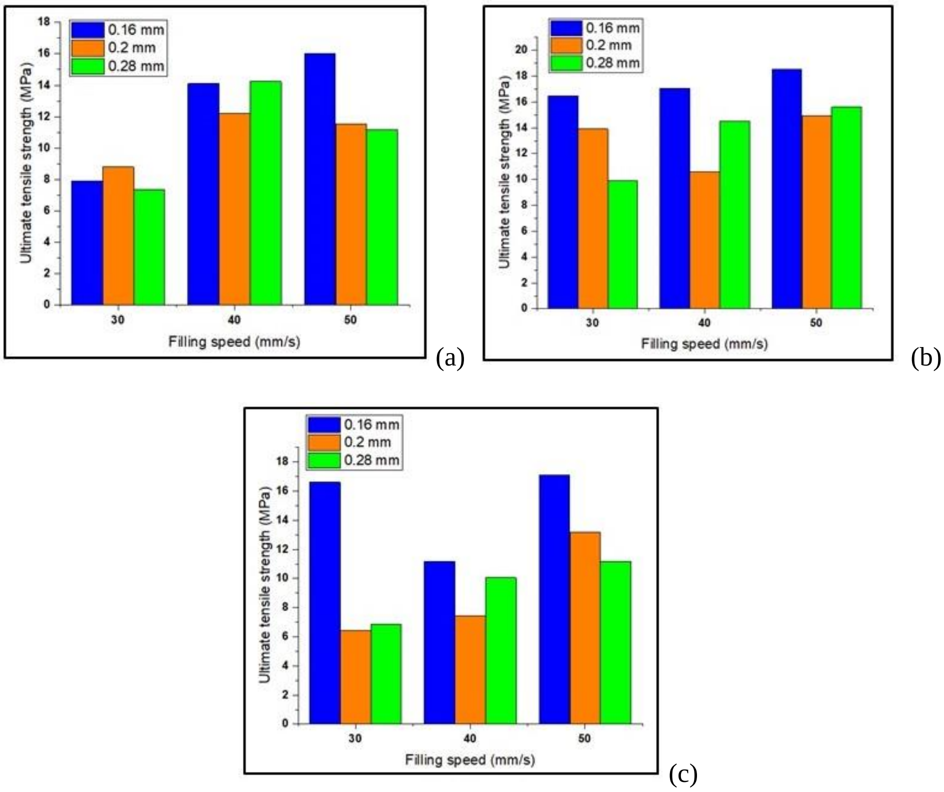

Figure 6. Ultimate tensile strength of 3D printed specimens (a) line (b) triangle and (c) gyroid

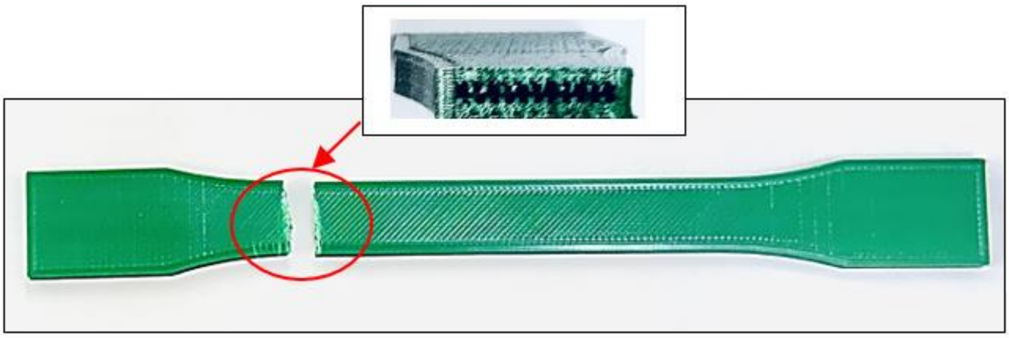

Figure 7. Brittle fracture in a tensile specimen

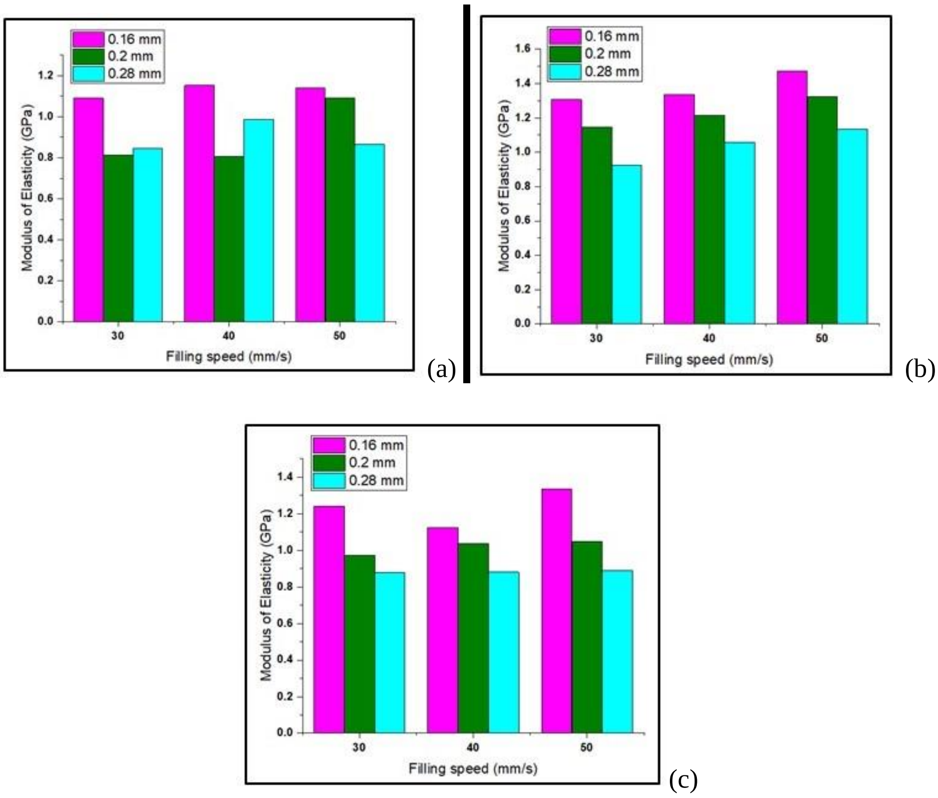

Figure 8. Modulus of Elasticity of 3D printed specimens (a) line (b) triangle and (c) gyroid

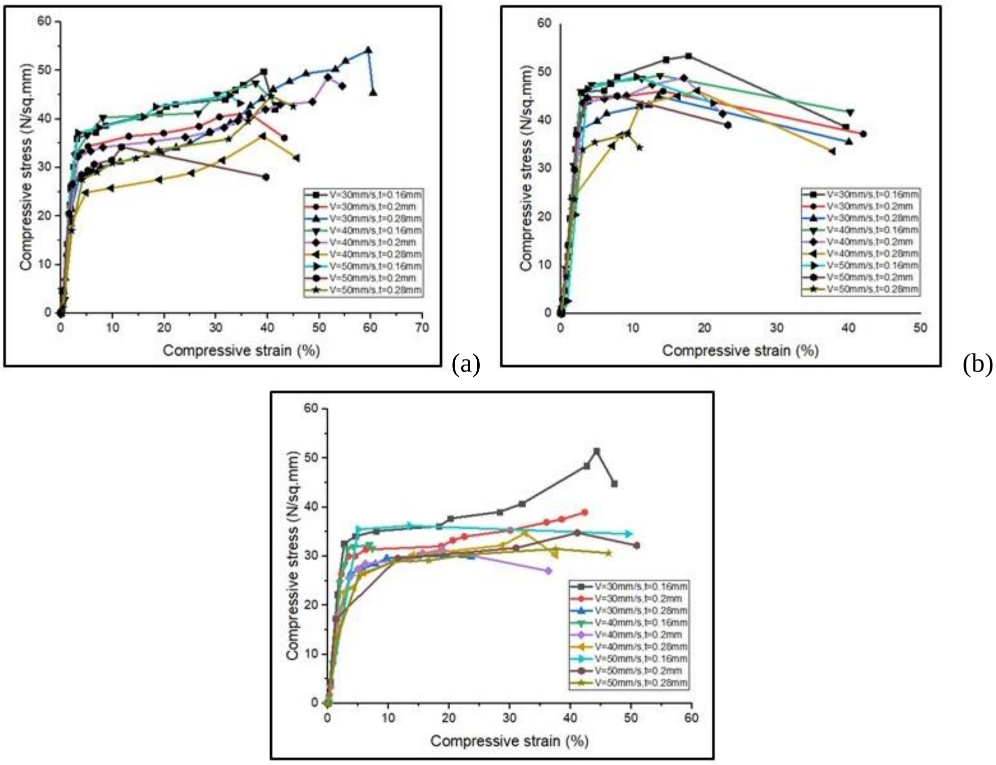

(c)

Figure 9. Compression stress-strain behavior of 3D printed specimens (a) line (b) triangle and (c) gyroid

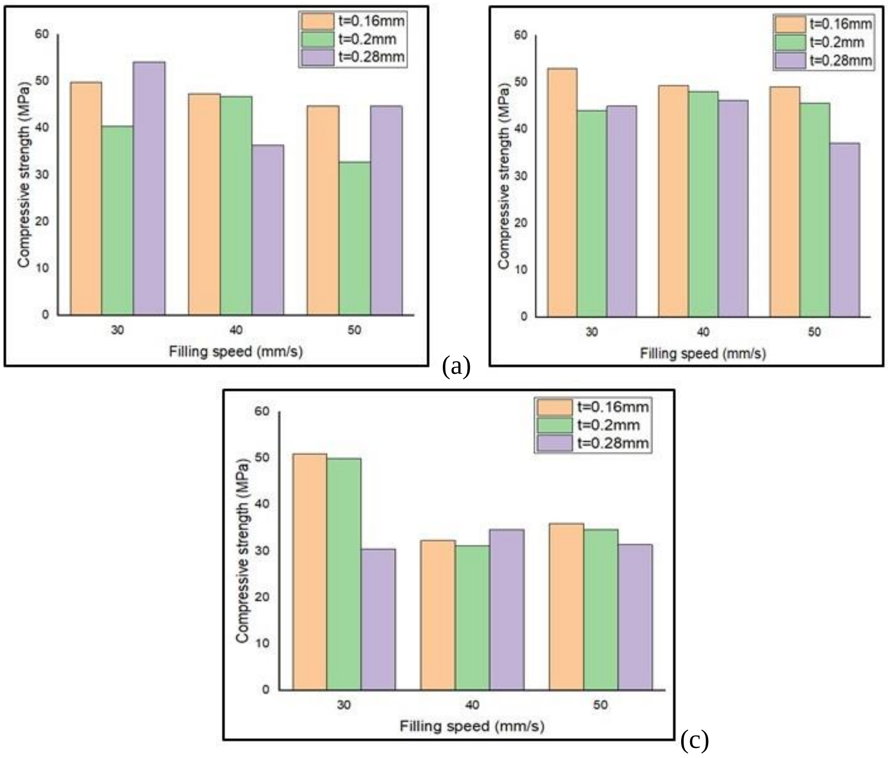

Figure 10. Compression strength of 3D printed specimens (a) line (b) triangle and (c) gyroid

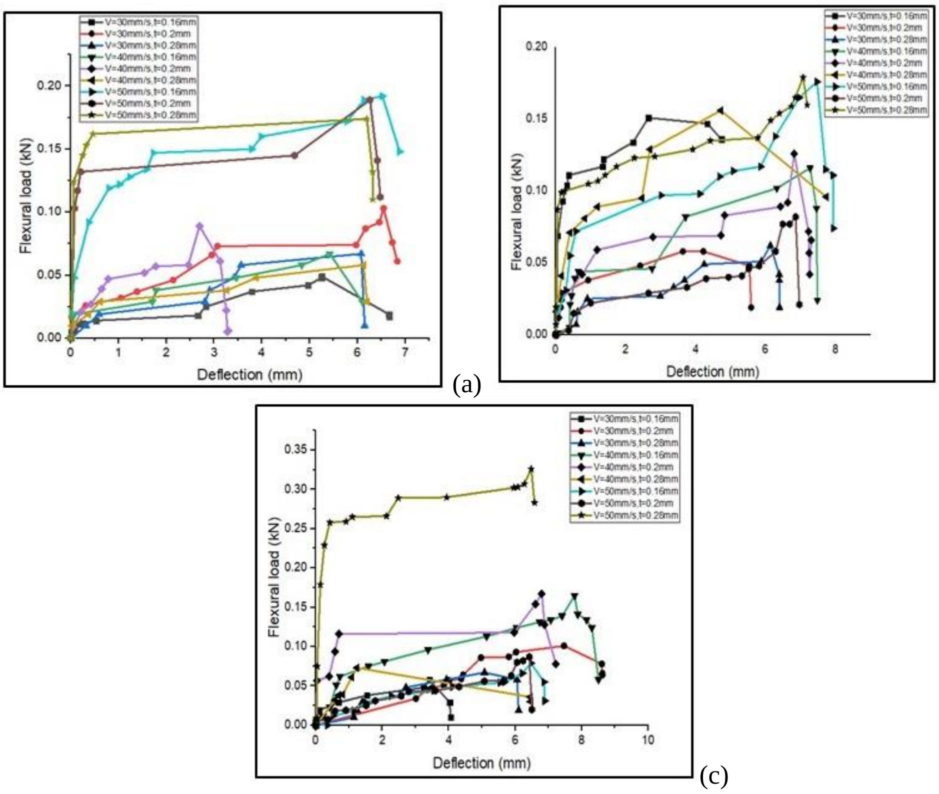

Figure 11. Flexural load capacity of 3D printed specimens (a) line (b) triangle and (c) gyroid

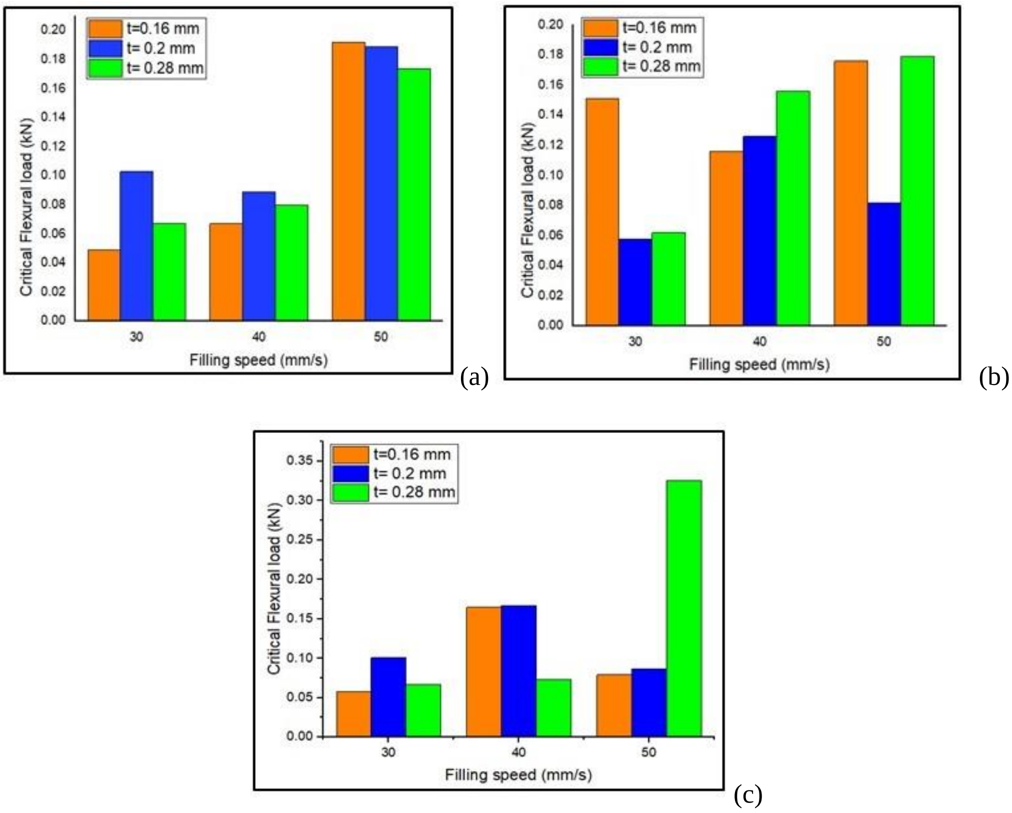

Figure 12. Flexural load capacity of 3D printed specimens (a) line (b) triangle and (c) gyroid

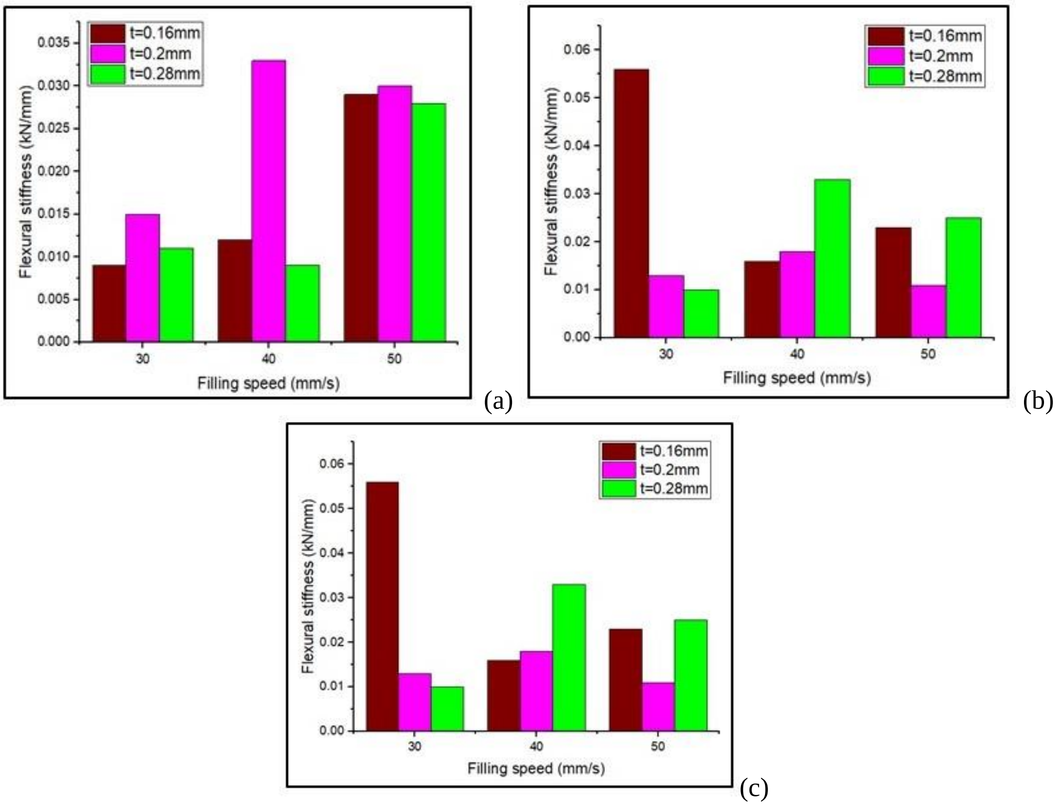

Figure 13. Flexural stiffness of 3D printed specimens (a) line (b) triangle and (c) gyroid

The variation of flexural load and its corresponding deflection on the sandwich composite laminate was shown in Figure 11 a-c plotted for different filling speeds, filling layer thicknesses and infill patterns. From the Figure 12 a-c, a drastic drop in critical flexural load was observed with increase in filling layer thickness from 0.16 mm to 0.28 mm (Torrado & Roberson, 2016). Influence of filling speed on the flexural load capacity seems to have a mixed effect i.e., higher flexural load capacity was observed at higher filling speed of 50 mm/s for line and triangular infill pattern whereas, in case of gyroid pattern, it was for 40 mm/s. This in turn confirmed that there was a significant influence of filling speed, filling layer thickness and infill pattern on the flexural behavior of the laminate. Higher filling speed during the fabrication of laminate resulted in reduced plasticity and lower filling layer thickness resulted in improved adhesion between the layers in the laminate. This was the reason for the corresponding flexural performance of the laminate (Gomez-Gras *et al*., 2017; Elkaseer *et al*., 2020; Kostakis *et al*., 2015). Higher void content in the gyroid pattern led to the drop in flexural load capacity at higher filling speed. Higher order flexural strength was noticed for triangular infill pattern compared to that of line and gyroid patterns. The reason may be attributed to the fact that the triangular structure was the strongest among others in terms of interlocking capacity and resistance towards the transverse loading. The deformation for the transverse loading was observed to be in the lower order for triangular pattern and which in turn resulted in significantly higher flexural strength in order to withstand the bending load capacities. The results obtained for flexural stiffness, shown in Figure 13 complemented the flexural load capacity irrespective of the process parameters.

Table 3. Parameters and their levels (coded)

PARAMETERS (un-coded)	**LEVEL (coded)**		
	-1	**0**	**+1**
Filling Speed (mm/s)	30	40	50
Infill Pattern	Line	Triangle	Gyroid
Layer Thickness (mm)	0.16	0.2	0.28

The input parameters, their type and performance indicators considered during optimization was shown in Table 3. The optimized multi parameters for the 3D printing were obtained using response optimizer tool in the Minitab software. It was found that the optimized process parameters with their levels highlighted were 30 mm/s filling speed, 0.16 mm filling layer thickness and triangular infill pattern. The composite desirability was 60.4 %, which was reasonably good. The influence of process parameters on the performance measures were shown by curves and dots in the Figure 14.

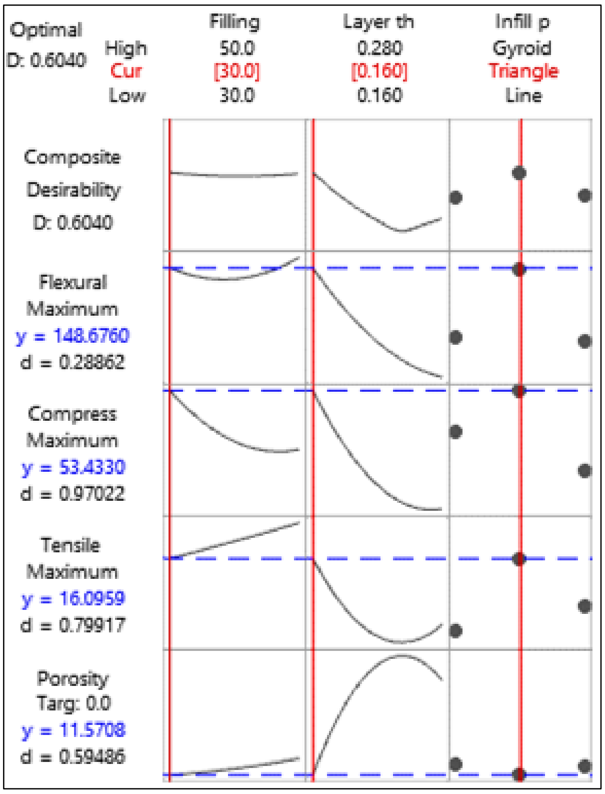

Figure 14. Response optimized parameters

4. Conclusions

The following conclusions were drawn from the investigation.

Higher order porosity was observed at layer thickness 0.28 mm and filling speed 50 mm/s. The tensile strength increased with an increase in the filling speed and a decrease in filling layer thickness. Least tensile strength of around 7 MPa was observed for specimen fabricated with the least filling speed of 30 mm/s and the minimum filling layer thickness of 0.16 mm. On the other hand, a maximum tensile strength of 15 MPa was observed for 50 mm/s filling speed and a layer thickness 0.16 mm. An increase in the filling speed during printing reduces the adhesion between the layers owing to insufficient bonding time, which in turn changes from plastic to elastic nature. The tensile performance of the specimens with the gyroid filling pattern was inferior to that of the line and triangular filling patterns because of poor interlocking capacity. Specimens fabricated with layer thickness 0.16 mm resulted in higher modulus of elasticity than that of other thickness irrespective of the filling pattern. Specimens fabricated with a filling speed of 30 mm/s and filling layer thickness of 0.16 mm resulted in better compressive strength than those fabricated with higher filling speed and filling layer thickness for all infill patterns. A higher filling speed during the fabrication of the laminate resulted in reduced plasticity and lower filling layer thickness resulted in improved adhesion between the layers in the laminate, thereby improving the flexural performance.

The above stated conclusions implied to the fact that all the three process parameters such as filling speed, layer thickness and infill pattern had influenced the mechanical behavior significantly and the optimized combination of process parameters for enhanced mechanical performance of 3D printed PLA specimens correspond to 0.16 mm layer thickness, 30 mm/s filling speed and triangular infill pattern. The important limitation of the present study was that the restriction of number of process parameters and their levels and maintained a constant nozzle temperature throughout the experiment as well. Inclusion of nozzle temperature and raster angle will be the future scope of this study to draw more results.

References

Al Khawaja, H., Alabdouli, H., Alqaydi, H., Mansour, A., Ahmed, W. & Hamad Al Jassmi, (2020). Investigating the mechanical properties of 3D Printed components. *Advances in Science and Engineering Technology International Conferences (ASET)*, 1-8.

Elkaseer, A., Schneider, S. & Scholz, S.G. (2020). Experiment-based process modeling and optimization for high-quality and resource-efficient FFF 3D printing. *Applied Sciences*, *10*(8), 2899.

Faidallah, R.F., Hanon, M.M., Szakál, Z. & Oldal, I. (2025). Mechanical characterization of 3D-Printed carbon fiber-reinforced polymer composites and pure polymers: Tensile and compressive behavior analysis. *International Review of Applied Sciences and Engineering*, *16*(1), 22-31.

Farbman, D., McCoy, C. (2016). Materials testing of 3D printed ABS and PLA samples to guide mechanical design. In *International Manufacturing Science and Engineering Conference*, 49903, V002T01A015. American Society of Mechanical Engineers.

Geng, P., Zhao, J., Wu, W., Ye, W., Wang, Y., Wang, S. & Zhang, S. (2019). Effects of extrusion speed and printing speed on the 3D printing stability of extruded PEEK filament. *Journal of Manufacturing Processes*, 37, 266-273.

Gomez-Gras, G., Jerez-Mesa, R., Travieso-Rodriguez, J.A. & Lluma, J. (2017). Fatigue performance of fused filament fabrication PLA specimens. *Materials & Design*, 140, 278-285.

Hanon, M.M., Marczis, R. & Zsidai, L. (2021). Influence of the 3D printing process settings on tensile strength of PLA and HT-PLA. *Periodica Polytechnica Mechanical Engineering*, *65*(1), 38-46.

Hodžić, D., Pandžić, A., Hajro, I. & Tasić, P. (2020). Strength comparison of FDM 3D printed PLA made by different manufacturers. *TEM J*, *9*(3), 966-970.

Kamer, M. S., Temiz, Ş., Yaykaşlı, H., Kaya, A. & Akay, O. (2022). Effect of printing speed on FDM 3D-printed PLA samples produced using different two printers. *International Journal of 3D Printing Technologies and Digital Industry*, *6*(3), 438-448.

Khan, S.F., Zakaria, H., Chong, Y.L., Saad, M.A.M. & Basaruddin, K. (2018). Effect of infill on tensile and flexural strength of 3D printed PLA parts. In *IOP Conference Series: Materials Science and Engineering*, *429*(1), 012101. IOP Publishing.

Kostakis, V., Niaros, V. & Giotitsas, C. (2015). Open source 3D printing as a means of learning: An educational experiment in two high schools in Greece. *Telematics and informatics*, *32*(1), 118-128.

Kun, K. (2016). Reconstruction and development of a 3D printer using FDM technology. *Procedia Engineering*, 149, 203-211.

Lanzotti, A., Grasso, M., Staiano, G. & Martorelli, M. (2015). The impact of process parameters on mechanical properties of parts fabricated in PLA with an open-source 3-D printer. *Rapid Prototyping Journal*, *21*(5), 604-617.

Letcher, T., Waytashek, M. (2014). Material property testing of 3D-printed specimen in PLA on an entry-level 3D printer. In *ASME International Mechanical Engineering Congress and Exposition*, 46438, V02AT02A014. American Society of Mechanical Engineers.

Liaw, C.Y., Tolbert, J.W., Chow, L.W. & Guvendiren, M. (2021). Interlayer bonding strength of 3D printed PEEK specimens. *Soft Matter*, *17*(18), 4775-4789.

Liu, J., Naeem, M.A., Al Kouzbary, M., Al Kouzbary, H., Shasmin, H.N., Arifin, N., ... & Abu Osman, N.A. (2023). Effect of infill parameters on the compressive strength of 3D-printed nylon-based material. *Polymers*, *15*(2), 255.

Liu, W., Zhou, J., Ma, Y., Wang, J. & Xu, J. (2017). Fabrication of PLA filaments and its printable performance. In *IOP Conference Series: Materials Science and Engineering*, *275*(1), 012033. IOP Publishing.

Mirkhalaf, S.M., Fagerström, M. (2021). The mechanical behavior of polylactic acid (PLA) films: Fabrication, experiments and modelling. *Mechanics of Time-Dependent Materials*, *25*(2), 119-131.

Misran, M.F.R., Othman, M.S. & Khamisan, Z.A.H. (2019). Study on mechanical properties of PLA printed using 3D printer. *Journal of Advanced Research in Applied Mechanics*, *59*(1), 10-18.

Nagaraju, D.S., Krupakaran, R.L., Sripadh, C., Nitin, G. & Emmanuel, G.J.J. (2023). Mechanical properties of 3D printed specimen using FDM (Fused deposition modelling) and SLA (Stereolithography) technologies. *Materials Today: Proceedings,* 1-15.

Naik, M., Thakur, D.G. (2021). Experimental investigation of effect of printing parameters on impact strength of the bio-inspired 3D printed specimen. *Sadhana*, *46*(3), 1-9.

Oksiuta, Z., Jalbrzykowski, M., Mystkowska, J., Romanczuk, E. & Osiecki, T. (2020). Mechanical and thermal properties of polylactide (PLA) composites modified with Mg, Fe, and polyethylene (PE) additives. *Polymers*, *12*(12), 2939.

Sedlak, J., Joska, Z., Jansky, J., Zouhar, J., Kolomy, S., Slany, M., ... & Jirousek, J. (2023). Analysis of the mechanical properties of 3D-printed plastic samples subjected to selected degradation effects. *Materials*, *16*(8), 3268.

Torrado, A.R., Roberson, D.A. (2016). Failure analysis and anisotropy evaluation of 3D-printed tensile test specimens of different geometries and print raster patterns. *Journal of Failure Analysis and Prevention*, 16, 154-164.

Xu, Z., Fostervold, R. & Razavi, N. (2021). Thickness effect on the mechanical behavior of PLA specimens fabricated via Fused Deposition Modeling. *Procedia Structural Integrity*, 33, 571-577.